8-1-2008

Evaluation of Advanced Adhesives for Aerospace Structures

P. Stoyanov

N. Rodriguez

T. Dickinson

D. H. Nguyen

E. Park

See next page for additional authors

Authors
P. Stoyanov, N. Rodriguez, T. Dickinson, D. H. Nguyen, E. Park, J. Foyos, V. Hernandez, J. Ogren, Michael Berg, and Omar S. Es-Said

JMEPEG (2008) 17:460–464
DOI: 10.1007/s11665-007-9158-4

1059-9495/$19.00

Evaluation of Advanced Adhesives for Aerospace Structures

P. Stoyanov, N. Rodriguez, T. Dickinson, D. Huy Nguyen, E. Park, J. Foyos, V. Hernandez, J. Ogren, M. Berg, and O.S. Es-Said

(Submitted June 28, 2007; in revised form July 12, 2007)

Polymer adhesives are finding increased use in panel joining applications in aircraft and aerospace structures where the applied stresses permit their use and where a uniform stress distribution is needed. One such adhesive, Hysol EA-9394™, was compared to three other formulations in this study. The new formulations were Hysol EA-9396, Hysol EA-9396 filled with nickel nanofibers and mixed by machine (Jamesbury Blender), and Hysol EA-9396 filled with nickel nanofibers and hand mixed in the laboratory. The comparison consisted of measuring shear lap strengths of aluminum test pieces bonded together with the candidate adhesives. The mechanical tests were supplemented by a Weibull analysis of the strength data and by a visual inspection of the failure mode (adhesive/cohesive). The lap shear strengths (fracture stress values) of all three Hysol EA-9396 adhesives were greater than that of the baseline Hysol EA-9394 polymer.

Keywords adhesive-bonding, failure statistics, joining, shear fracture, Weibull analysis

1. Introduction

The procedures available for joining aluminum panels are limited due to the reactivity of molten aluminum in ambient atmospheres. In the cases of aluminum alloys, the benefits of prior aging treatments are lost in the heat-affected zone (HAZ) because the thermal environment causes over-aging. Rivets and related fasteners are possibilities, but can produce regions of stress concentrations. Low-density adhesives have been employed to join panels of aluminum thin plates (Ref 1), and continuous effort exists to improve their performance.

The purpose of this study was to determine if three modifications of a baseline adhesive, Hysol EA-9394, showed improved properties over that baseline. This evaluation consisted of measuring the lap shear strengths at room temperature of a statistically significant number of identical test samples in order to develop failure statistics.

2. Experimental

One adhesive, Hysol EA-9394™ (Ref 2) was taken in this study to be the baseline standard and compared to the three variations, i.e.:

Hysol EA 9396
Hysol EA-9396 + nickel nanofibers blended with a Jamesbury Blender
Hysol EA-9396 + nickel nanofibers blended by hand

Both Hysol EA-9394 and 9396 are curable two-part polymers produced by condensation reactions. They differ in that Part A in EA-9394 is an epoxy resin while Part A in EA-9396 is an amine (Ref 3). Both cure in 2 to 4 days at ambient conditions.

The nickel nanofiber loading was the same in both cases.

The test activity described in this article excluded detailed data on the nickel nanofibers; their characteristics and their volumetric loading fractions.

The aluminum strip sample geometry is shown in Fig. 1. In that figure:

(i) a and c are the measured test strip thickness values.
(ii) $(a + c)$ is the bond thickness.
(iii) $d \times w$ is the bond area.

No strain was observed in the aluminum strips.

Lap shear tests were performed on an Instron 4505 universal testing machine. A load cell indicated the force at fracture. Computer software calculated the fracture stress from the load and the dimensions of the lap joint. All the tests were performed under ambient condition; ~25 °C (77 °F) and nominally 60 to 80% relative humidity. Thirty samples of each of the four formulations (baseline + three modifications) were tested.

3. Results

Shear lap stress results for all 120 samples are summarized in Table 1. Fracture stress values for all samples are shown in Tables 2 to 5.

P. Stoyanov, N. Rodriguez, T. Dickinson, D. Huy Nguyen, E. Park, J. Foyos, J. Ogren, and **O.S. Es-Said**, Mechanical Engineering Department, Loyola Marymount University, Los Angeles, CA 90045; **V. Hernandez**, Northrop Grumman Space Technology, Redondo Beach, CA 90278; **M. Berg**, Mathematics Department, Loyola Marymount University, Los Angeles, CA 90045. Contact e-mail: oessaid@lmu.edu.

™Hysol is a trademark of the Henkel Corporation.

4. Discussion

The data show a wide range of fracture stresses for ostensibly identical samples. The data warranted an analysis according to the method of Weibull (Ref 4, 5). In this analysis, it is assumed that a "weak link" exists where failure (fracture in this case) originates. The following equation stems from the analysis:

$$\ln\left[\ln\left(\frac{1}{P_s}\right)\right] = \text{constant} + m \ln \sigma_F \qquad \text{(Eq 1)}$$

where P_s = probability that a sample will survive at stress of σ_F and m = slope of the $\ln[\ln(1/P_s)]$ versus $\ln \sigma_F$ curve. All the test samples had the same volume.

The Weibull plots, based on the data in Tables 2 to 5, are in Fig. 2.

All four adhesive samples exhibit linear plots. Linear regression analyses for the four adhesives yielded:

$$\ln\left[\ln\left(\frac{1}{P_s}\right)\right] = -20.8 + 6.8 \ln \sigma_F \qquad \text{(Eq 2)}$$

Hysol EA-9394 (baseline)

$$\ln\left[\ln\left(\frac{1}{P_s}\right)\right] = -41.5 + 12.2 \ln \sigma_F \qquad \text{(Eq 3)}$$

Hysol EA-9396

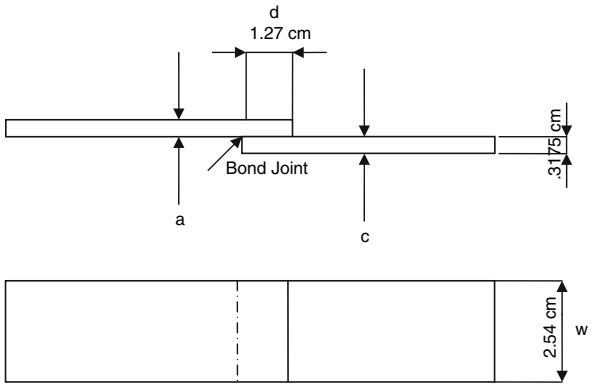

Fig. 1 Test sample configuration (dimensions in cm)

$$\ln\left[\ln\left(\frac{1}{P_s}\right)\right] = -27.6 + 8.4 \ln \sigma_F \qquad \text{(Eq 4)}$$

Hysol EA-9396 (hand mixing)

$$\ln\left[\ln\left(\frac{1}{P_s}\right)\right] = -50.4 + 14.6 \ln \sigma_F \qquad \text{(Eq 5)}$$

Hysol EA-9396 (machine mixing)

From a design standpoint, a steep (almost vertical) curve is preferred. The data in Fig. 2 clearly indicates that the steepest curve (largest slope) was for the machine-mixed Hysol EA-9396 containing nickel nanofibers.

Table 2 Fracture data of Hysol EA-9394

Sample	Fracture stress, psi/MPa		Bondline thickness, in./cm	
EA 1	3309	23	0.014	0.036
EA 2	3007	21	0.011	0.028
EA 3	3553	25	0.013	0.033
EA 4	3521	24	0.009	0.023
EA 5	3036	21	0.012	0.030
EA 6	2354	16	0.015	0.038
EA 7	2002	14	0.011	0.028
EA 8	2090	14	0.017	0.043
EA 9	3274	23	0.011	0.028
EA 10	2715	19	0.011	0.028
EA 11	3396	23	0.012	0.030
EA 12	3370	23	0.013	0.033
EA 13	2218	15	0.012	0.030
EA 14	3244	22	0.013	0.033
EA 15	3441	24	0.010	0.025
EA 16	2816	19	0.012	0.030
EA 17	2160	15	0.014	0.036
EA 18	3076	21	0.009	0.023
EA 19	2607	18	0.010	0.025
EA 20	2984	21	0.012	0.030
EA 21	2409	17	0.009	0.023
EA 22	3256	23	0.014	0.036
EA 23	2721	19	0.013	0.033
EA 24	3129	22	0.006	0.015
EA 25	3108	21	0.010	0.025
EA 26	2935	20	0.009	0.023
EA 27	2609	18	0.007	0.018
EA 28	2852	20	0.013	0.033
EA 29	2763	19	0.012	0.030
EA 30	2784	19	0.008	0.020

1 Ksi = 6.89 MPa

Table 1 Shear lap stress results

Adhesive/Polymer	Minimum fracture shear stress		Maximum fracture shear stress		Average fracture shear stress	
	psi	MPa	psi	MPa	psi	MPa
Hysol EA-9394	2000	13.8	3560	24.5	2890	19.2
Hysol EA-9396	3290	22.7	4800	33.1	4190	28.8
Hysol EA-9396 plus machine-mixed nickel nanofibers	3750	25.8	5070	34.9	4390	30.2
Hysol EA-9396 plus hand-mixed nickel nanofibers	1530	10.6	460	31.3	3660	25.2

Table 3 Fracture data for Hysol-EA 9396

Sample	Fracture stress, psi/MPa		Bondline thickness, in./cm	
EB 1	4201	29	0.004	0.010
EB 2	4662	32	0.011	0.028
EB 3	3819	26	0.007	0.018
EB 4	4527	31	0.006	0.015
EB 5	4800	33	0.004	0.010
EB 6	4153	29	0.012	0.030
EB 7	4383	30	0.013	0.033
EB 8	3812	26	0.013	0.033
EB 9	4191	29	0.012	0.030
EB 10	4392	30	0.010	0.025
EB 11	3976	27	0.008	0.020
EB 12	4322	30	0.008	0.020
EB 13	3887	27	0.011	0.028
EB 14	4358	30	0.004	0.010
EB 15	4440	31	0.010	0.025
EB 16	4000	28	0.003	0.008
EB 17	4450	31	0.007	0.018
EB 18	3515	24	0.011	0.028
EB 19	4195	29	0.007	0.018
EB 20	4350	30	0.006	0.015
EB 21	4428	31	0.006	0.015
EB 22	4379	30	0.008	0.020
EB 23	3291	23	0.012	0.030
EB 24	4386	30	0.007	0.018
EB 25	3716	26	0.007	0.018
EB 26	4526	31	0.005	0.013
EB 27	4228	29	0.010	0.025
EB 28	3593	25	0.012	0.030
EB 29	4504	31	0.009	0.023
EB 30	4085	28	0.007	0.018

1 Ksi = 6.89 MPa

All fractures for this formulation were above 26 MPa (3750 psi), whereas virtually all the samples using Hysol EA-9394™ fractured at values below that value of shear stress.

The fractures were virtually always cohesive in nature with both fracture surfaces covered with adhesive. A few anomalous samples were found in which the fractures were mixed mode, i.e., portions of the fracture surfaces were bare. The anomalous surfaces are in Fig. 3 along with a normal surface. The anomalous surfaces shown in Fig. 3 correspond to the four anomalous low fracture stress values in Fig. 2.

The anomalous low fractures occurred with the adhesive that contained nickel nanofibers that had been hand mixed into the liquid adhesive.

This fact leads to the hypothesis that the hand mixing operation, per say, did not result in a uniform adhesive. The surface preparation of the aluminum surfaces certainly was satisfactory because all of the other fractures occurred within the adhesive.

Further analysis of the data in Tables 2 to 5 indicates that the fracture stress did not depend on adhesive thickness, within the range of measured thickness values, Fig. 4 to 7.

The data generated in this study can be compared with data obtained in previous studies.

The data sheets for EA 9394 for tensile lap shear strength at 77 °F (25 °C) give 28.9 MPa as the value for bonds involving 2024-T3 aluminum alloy treated with phosphoric acid as a surface preparation procedure (Ref 2). The comparable number for EA 9396 is 27.6 MPa (Ref 3).

Both values are for the adhesive without re-enforcing nickel nanofibers.

Table 4 Fracture data for Hysol EA-9396 containing hand-mixed nickel nanofibers

Sample	Fracture stress, psi/MPa		Bondline thickness, in./cm	
EBXM 1	3031(a)	21	0.006	0.015
EBXM 2	4028	28	0.008	0.020
EBXM 3	3381	23	0.008	0.020
EBXM 4	3372	23	0.007	0.018
EBXM 5	2702(a)	19	0.006	0.015
EBXM 6	3700	26	0.010	0.025
EBXM 7	3439	24	0.011	0.028
EBXM 8	3666	25	0.012	0.030
EBXM 9	4067	28	0.009	0.023
EBXM 10	4546	31	0.010	0.025
EBXM 11	3874	27	0.009	0.023
EBXM 12	3698	26	0.012	0.030
EBXM 13	3540	24	0.010	0.025
EBXM 14	4085	28	0.012	0.030
EBXM 15	3968	27	0.010	0.025
EBXM 16	4340	30	0.010	0.025
EBXM 17	4082	28	0.008	0.020
EBXM 18	4186	29	0.011	0.028
EBXM 19	4419	31	0.007	0.018
EBXM 20	4127	29	0.010	0.025
EBXM 21	2159(a)	15	0.009	0.023
EBXM 22	3840	27	0.013	0.033
EBXM 23	3439	24	0.010	0.025
EBXM 24	3013	21	0.010	0.025
EBXM 25	1534(a)	11	0.010	0.025
EBXM 26	3759	26	0.009	0.023
EBXM 27	3770	26	0.008	0.020
EBXM 28	3400	23	0.010	0.025
EBXM 29	4174	29	0.010	0.025
EBXM 30	4354	30	0.009	0.023

1 Ksi = 6.89 MPa
(a) Samples failed in an adhesive mode

None of the simple EA 9394 samples reached such fracture stress values.

Several EA 9396 samples reached such values. However, using the linear regression analysis of the experimental data, it is seen that a survival rate of approximately 30% might be expected at 27.6 MPa.

It is speculative to compare the properties of the simple (nonnickel nanofiber) polymer with those that had been re-enforced with nickel fibers. Suffice it to state that the machine-mixed EA 9396 might be expected to have a survival rate of 85% if exposed to a stress of 27.6 MPa.

Previous work had shown that the butt strength depended on bond thickness (Ref 6). However, all the bonds in the Guess-Reedy-Stavig study were much thicker than those used in the present study. Also, the dependence found in that study was weak at best.

5. Conclusions

One adhesive formulation, Hysol EA-9396 containing machine-mixed nickel nanofibers, required the largest stress to cause fracture. Furthermore, from an engineering failure control standpoint, this formulation was superior to the others because fracture (failure) occurred over the smallest range of stress values; hence it provided the smallest margin of uncertainty in failure control.

The test results show that the Hysol EA-9396 warrants further examination; in particular, the effect of test temperature on fracture shear stress.

Table 5 Fracture data for Hysol EA-9396 containing machine-mixed nickel nanofibers

Sample	Fracture stress, psi/MPa		Bondline thickness, in./cm	
EBX 1	4376	30	0.011	0.028
EBX 2	4564	32	0.011	0.028
EBX 3	4260	29	0.012	0.030
EBX 4	4593	32	0.012	0.030
EBX 5	4429	31	0.012	0.030
EBX 6	4863	34	0.013	0.033
EBX 7	3750	26	0.013	0.033
EBX 8	4493	31	0.014	0.036
EBX 9	4778	33	0.014	0.036
EBX 10	4276	30	0.013	0.033
EBX 11	4573	32	0.009	0.023
EBX 12	4268	29	0.011	0.028
EBX 13	4169	29	0.012	0.030
EBX 14	4252	29	0.013	0.033
EBX 15	5066	35	0.009	0.023
EBX 16	4413	30	0.009	0.023
EBX 17	4171	29	0.010	0.025
EBX 18	4329	30	0.011	0.028
EBX 19	3931	27	0.011	0.028
EBX 20	4752	33	0.007	0.018
EBX 21	4541	31	0.008	0.020
EBX 22	4752	33	0.009	0.023
EBX 23	4639	32	0.012	0.030
EBX 24	4819	33	0.012	0.030
EBX 25	4281	30	0.007	0.018
EBX 26	3990	28	0.009	0.023
EBX 27	4169	29	0.009	0.023
EBX 28	4126	29	0.013	0.033
EBX 29	3953	27	0.010	0.025
EBX 30	4072	28	0.008	0.020

1 Ksi = 6.89 MPa

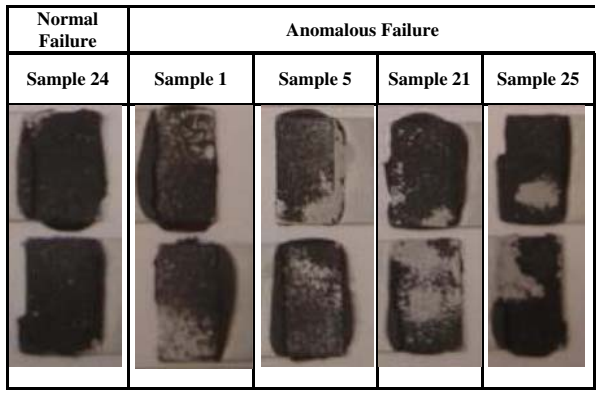

Fig. 3 Post-test fracture surfaces: Sample 24 is the sample identified in Table 5 as EBX-24. Samples 1, 5, 21, and 25 are the starred samples in Table 4 and all exhibited low fracture shear stresses

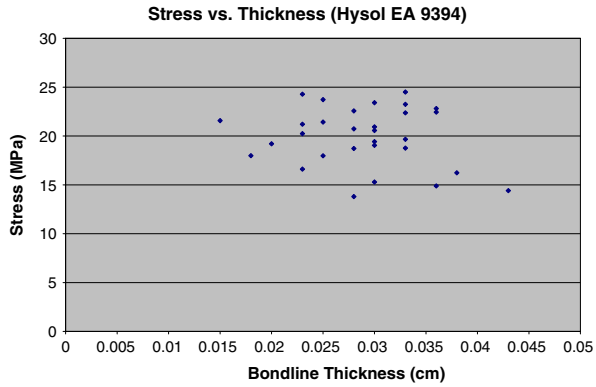

Fig. 4 Fracture stress versus adhesive bondline thickness for Hysol EA-9394

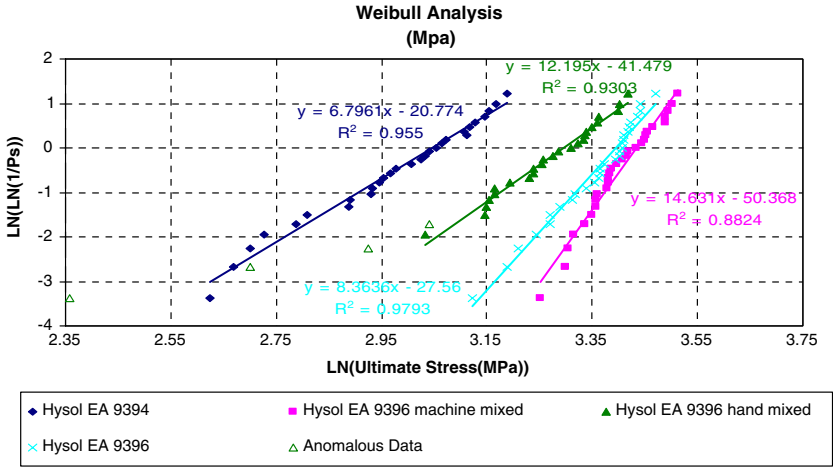

Fig. 2 Weibull curves for all four groups of adhesively bonded joints. The hand-mixed samples contain four anomalous data points discussed elsewhere in this article

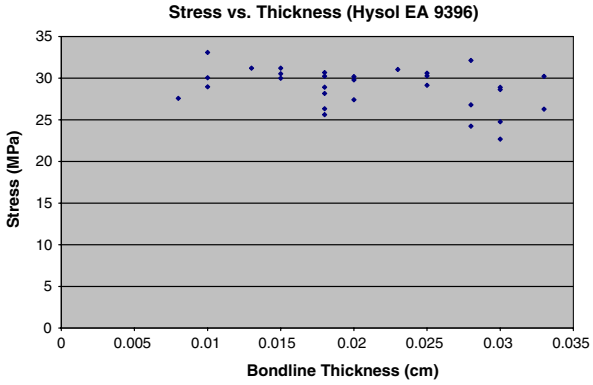

Fig. 5 Fracture stress versus adhesive bondline thickness for Hysol EA-9396

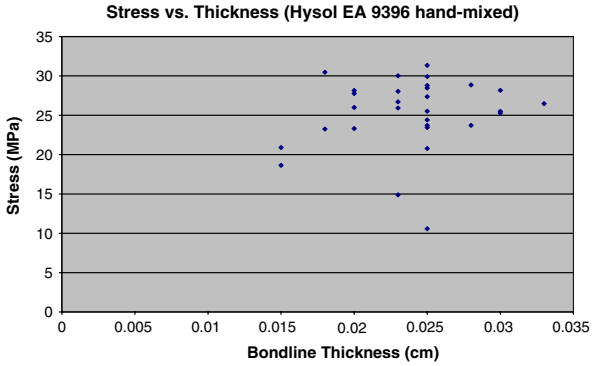

Fig. 6 Fracture stress versus adhesive bondline thickness for Hysol EA-9396 containing hand-mixed nickel nanofibers

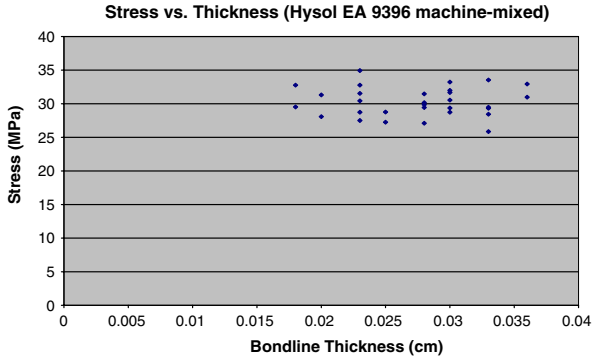

Fig. 7 Fracture stress versus adhesive bondline thickness for Hysol EA-9396 containing machine-mixed nickel nanofibers

Acknowledgments

The authors wish to thank the National Science Foundation (NSF) Grant Research No. EEC0353668 Experience for Undergraduates (REU) program. Ms. Esther Bolding is the manager of this program.

References

1. T. Gaston, Building a Better Adhesive Bond, *Machine Design*, 2003, http://www.machinedesign.com/asp
2. Anon, Hysol EA 9394, Retrieved from Henkel Corporation in Aerospace Group, 2002, http://www.loctiteaero.comp/Images/Datasheet_PDF/Hysol_EA_9394.pdf
3. Anon, Hysol EA 9396, Retrieved from Henkel Corporation Aerospace Group, 2002, http://www.loctiteaero.com/Images/Datasheet_PDF/Hysol_EA 9396.pdf
4. W. Weibull, A Statistical Distribution Function of Wide Applicability, *J. Appl. Mechanics*, 1951, **18**, p 293–297
5. D. Hull and T.W. Clyne, An Introduction to Composite Materials, 2nd edition, Cambridge University Press (1996)
6. T.R. Guess, E.D. Reedy, and M.E. Stavig, Mechanical Properties of Hysol EA-9394 Structural Adhesive, SAND 0229, Feb 1995